DEVELOPMENT OF 3D FEM PROGRAM FOR SIMULATION OF RETINA DETACHMANT OPERATION ON AN EYEBALL TOWARD PRACTICAL USE

Zhi-Gang SUN* and Akitake MAKINOUCHI†

* Division of Computer and Information, RIKEN
† Integrated V-CAD System, RIKEN
2-1 Hirosawa, Wako-shi, Saitama 351-0198, Japan
e-mail: *zgsun@postman.riken.go.jp
†akitake@postman.riken.go.jp

Abstract: Scleral buckling operation is one of the surgeries that most frequently performed in clinic to treat the retinal detachment on an eyeball. However, the effect of the operation strongly depends on the surgeon's experience and it is usually difficult to obtain a satisfactory operation effect in the clinic. So the computer-aided surgery planning is now greatly desired. In order to meet such a desire from the surgeon, we have been developing a 3-D FEM program for coupling analysis of the incompressible hyperelastic solid and static liquid. In this paper, a new solid-liquid coupling analysis algorithm was proposed to improve its calculation efficiency and to solve its memory-expensive problem in order to make its practical use possible. Furthermore, the contact treatment function between deformed bodies, which is necessary to treat the contact between the detached retina and choriod, was further implemented. The program, thus, has now already possessed all the functions needed for the numerical simulation of the buckling operation. Finally, a simulation of the encircling buckling operation was carried out and the results demonstrated the ability of the program to predict the suitable factors for a effective operation, such as buckle shape, buckle location, buckling strength, suture width, Suture strength and so on.

1. INTRODUCTION

The eyeball is a complex 3D structure consisting of over ten types of living tissues, including both soft tissues and liquid tissues. The retina is the light-sensitive tissue that turns light signal into visual information sent to the brain. It is very similar to film in a camera. In a healthy eyeball, the retina always adheres to the choriod and thus the human's normal vision is guaranteed. However, as the retina separates from the choriod due to vitreous liquefying, injury etc., the retina detachment occurs and, it will cause impairment or even loss of the vision. In that case, a surgery is required to perform in order to improve the vision. There are several types of surgery in the clinic to treat the retinal detachment disease. One of them is the scleral buckling operation. In this procedure, the wall of the eyeball where the retina detaches is indented by stitching a silicon tire to the sclera's surface directly or after the eyeball is buckled up by a silicon band, which are respectively called the segmental buckling operation and the encircling buckling operation, to reattach the detached retina.

Although this procedure is a theoretically effective operation and it is the most common one in

use today, it is usually difficult to obtain a desired operation effect and its success rate is not so high at present, because it demands excellent skill of an experienced surgeon. In other word, the effect of this operation procedure strongly depends on the surgical experience at present. In such a background, the computer-aided surgery planning is now greatly desired in the clinic. The biomechanical simulation employing the finite element method is a useful means to meet this desire and it is expected that the simulation in advance can predict suitable factors for a desired operation, which govern the operation effect such as buckle shape, buckle location, buckling strength, suture width, Suture strength and so on.

As mentioned above, the eyeball is consisted of both the soft tissue and liquid tissue, and the scleral buckling operation is a very complicated procedure. As a numerical simulation application, thus, it is a quite difficult case due to the fact that it includes strong geometrical, material and contact nonlinearities as well as the problems of the solid-liquid coupling analysis and of the suture treatment etc.. To enable this simulation, we have developed a 3D FEM program[1][2] for coupling analysis of the incompressible hyperelastic solid and static liquid, in which the contact treatment between the deformed body and rigid body was available. In this paper, a new coupling analysis algorithm is proposed to further improve its analysis efficiency and to solve its memory-expensive problem. Furthermore, the functions of the contact treatment between the deformed bodies and of the suture treatment, which are necessary to treat the contact between retina and choriod and to simulate the suture process, is newly introduced. The program thus now possesses all the functions required by a simulation of the scleral buckling procedure as shown below.

Functions of the 3D FEM program:

1) Available element type: 3D hexahedral mixed element with eight displacement nodes and one pressure node.
2) Available boundary conditions: nodal displacement, nodal force and pressure.
3) Coupling analysis for incompressible hyperelastic solid and static liquid.
4) Available strain energy function of the hyperelastic solid: $W = \sum_{r,s\geq 0} c_{rs}(I_1 - 3)^r (I_2 - 3)^s$
5) Contact treatment between the deformed body and rigid body.
6) Contact treatment between the deformed bodies.
7) Suture treatment.

To demonstrate the ability of this program, an actual encircling buckling operation is simulated using an eyeball model in which the retinal detachment is definitely described and the results are given.

2. NUMERICAL METHOD

2.1 A new FEM formulation for coupling analysis of the incompressible hyperelastic solid and static liquid

The mixed finite element method based on the total Lagrange formulation is employed for analysis of the incompressible hyperelastic solid. The total potential energy function is defined in the following form:

$$\Phi = \int_{V0} [W(\bar{I}_1, \bar{I}_2) + 2\lambda(J-1)]dV - g(u) \tag{1}$$

where W is the strain energy function expressed by I_1 and I_2, the reduced invariants of the right Cauchy-Green deformation tensor; λ is the Lagrange multiplier; J is the determinant of the Jacobian matrix; V_0 is the volume of deformation body in the reference configuration; $g(u)$ is the potential energy of external force; u is the displacement.

Invoking the stationary of (1), the variation of the potential energy can be expressed as:

$$\delta\Phi = \int_{V0} [\partial W / \partial \varepsilon_{ij} + 2\lambda(\partial J / \partial \varepsilon_{ij})]\delta\varepsilon_{ij} dV + \int_{V0} 2(J-1)\delta\lambda dV - (\partial g / \partial u)\partial u = 0 \tag{2}$$

Thus, The equilibrium equation for an element can be obtained by discretizing the above variational equation as

$$\begin{cases} \int_{V0} [\partial W / \partial \varepsilon_{ij} + 2\lambda(\partial \lambda / \partial \varepsilon_{ij})][(\partial \phi_N / \partial X_j)u_{Nk} + \delta_{jk}](\partial \phi_M / \partial X_i)dV = r_{Mk} \\ \int_{V0} \varphi_L 2(J-1)dV = 0 \end{cases} \tag{3}$$

where ε_{ij} denotes the Green-Lagrange strain; u_{Nk} the node displacement; X_i the initial node coordinate at the reference configuration; ϕ and ψ the interpolations of displacement and Lagrange multiplier; r_{Mk} the equivalent nodal force corresponding to $g(u)$ in (1).

In the solid-liquid coupling analysis, the nodal forces equivalent to the liquid pressure, which acts on an quadrilateral element lying on the solid-liquid interface and changes continually during deformation, can be derived out as follows (refer to [1] for detail):

$$\boldsymbol{r}_e^L = \int_{S0} \boldsymbol{\Phi}^T P^L J \boldsymbol{F}^{-T} \boldsymbol{n}_0 dS \qquad J = det|\boldsymbol{F}| \tag{4}$$

where $\boldsymbol{\Phi}$ is the matrix composed of interpolation functions of the quadrilateral element; $\boldsymbol{F}$ is the deformation gradient; $\boldsymbol{n}_0$ and s_0 are the inward normal of element and the element area at reference configuration and P is the liquid pressure at current configuration calculated by

$$P^L = P_{ini}^L + \Delta P^L = P_{ini}^L - K\frac{V^L - V_{ini}^L}{V_{ini}^L} \tag{5}$$

P_{ini} and V_{ini} are the initial liquid pressure and the initial liquid volume; V is the current liquid volume; K is the liquid bulk modulus.

Thus, by substituting (4) into the right-hand side of the first equation in (3), paying attention to node correspondence, the equilibrium equations of an element with a side on the solid-liquid interface for the coupling analysis can be obtained as follows,

$$\begin{cases} \int_{V0} [\partial W / \partial \varepsilon_{ij} + 2\lambda(\partial \lambda / \partial \varepsilon_{ij})][(\partial \phi_N / \partial X_j) u_{Nk} + \delta_{jk}](\partial \phi_M / \partial X_i) dV = r_{Mk}^O + r_{Mk}^L \\ \int_{V0} \varphi_L \, 2(J-1) dV = 0 \end{cases} \tag{6}$$

where r_{Mk}^L is the component of $\boldsymbol{r}_e^L$ in (4) and r_{Mk}^O is the others.

In the previous formulation[1], it is after substituting (5) into (4) to perform this procedure so that the nonzero terms in the stiffness matrix significantly increase because the liquid pressure is related to displacements of all the nodes on the solid-liquid interface. This can results in a long time and a large memory needed for the analysis in the case of using the sparse solver to solve the stiffness equation. To improve this disadvantage, in the new formulation, The liquid pressure is used as a unknown variable and the relation(5) is directly added to the equilibrium equation set to couple the liquid with the solid as shown below.

$$\begin{cases} f_{ij}(u_{11}, u_{12}, u_{13,} \cdots, u_{n1}, u_{n2}, u_{n3}, \lambda_1, \cdots, \lambda_m) = r_{ij}^O & \text{for the nodes not lying on the interface.} \\ f_{ij}(u_{11}, u_{12}, u_{13,} \cdots, u_{n1}, u_{n2}, u_{n3}, \lambda_1, \cdots, \lambda_m) = r_{ij}^O + r_{ij}^L(P^L) & \text{for the nodes lying on the interface.} \\ f_{3n+l}(u_{11}, u_{12}, u_{13,} \cdots, u_{n1}, u_{n2}, u_{n3}) = 0 & \\ p^L - (p_{ini}^L + \Delta p^L(u_{11}^{ps}, u_{12}^{ps}, u_{13}^{ps}, \cdots, u_{k1}^{ps}, u_{k2}^{ps}, u_{k3}^{ps})) = 0 & \end{cases} \tag{7}$$

$i = 1,n \qquad j = 1,3 \qquad l = 1,m$

where *n* and *m* denote the total number of node and element. *k* denotes the number of the nodes lying on the solid-liquid interface.

By linearizing (7) using the Taylor series expansion, the global incremental stiffness equation for the Newton-Raphson iteration scheme is finally obtained in the following form:

$$\begin{bmatrix} \boldsymbol{K}_u^{i-1} & \boldsymbol{K}_\lambda^{i-1} & \boldsymbol{K}_p^{i-1} \\ \boldsymbol{K}_\lambda^{i-1T} & & \\ \boldsymbol{K}_p^{i-1T} & \boldsymbol{0} & \end{bmatrix} \begin{bmatrix} \Delta \boldsymbol{U}^i \\ \Delta \boldsymbol{\lambda}^i \\ \Delta \boldsymbol{P}^i \end{bmatrix} = \begin{bmatrix} \boldsymbol{FU}^{i-1} \\ \boldsymbol{F\lambda}^{i-1} \\ \boldsymbol{FP}^{i-1} \end{bmatrix} + \begin{bmatrix} \boldsymbol{R} \\ \boldsymbol{0} \\ \boldsymbol{0} \end{bmatrix} \tag{8}$$

From the above (7) and (8), it is clear that the number of nonzero terms in the stiffness matrix which increased due to introduction of the liquid is $2 \times 3k+1$ and it greatly decreased compared to the previous formulation, in which it is approximately $3k \times 3k$. Using the new formulation proposed here, thus, an efficient and large-scale coupling analysis will be possible.

2.2 Suture treatment

In order to simulate the suture process, a straightforward way is adopted in the program. As shown in Fig 1, during the suture process in the sclera buckling operation, a buckle called silicon

tire is stitched to the surface of the eyeball by slowly pulling suture strings along the buckle surface as well as within the planes normal to the generator of the buckle surface. Therefore, this process can be considered as an alternative process in which the suture points on the eyeball surface are continuously subjected to the nodal forces in the tangent directions to the outlines of the buckle cross sections which lie on the same planes as suture points. In this program, thus, the calculations in each steps was performed under the nodal force boundary conditions enforced to the suture points in such directions, which are sought out in last calculation step, to pursue the suture process.

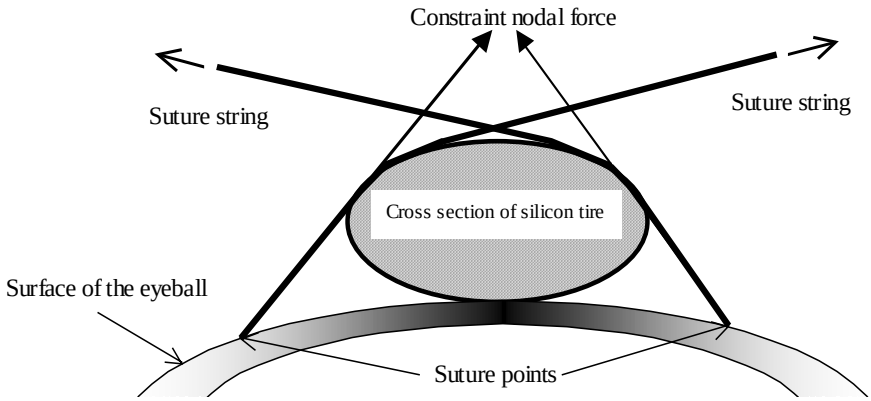

Fig.1 Suture process in the scleral buckling operation

2.3 Contact treatment between the deformed bodies

2.3.1 Specification and description of the contact surface

The contact surface pair consisting of two surfaces, being called a master surface and a slave surface, which have potential to contact with each other during deformation are firstly specified. In this program, the master surface are then described in triangular meshes obtained by subdividing the quadrilateral meshes that are sides of the hexahedral elements using to analysis so that the iteration calculation for finding the natural coordinates of the target points in the case of using quadrilateral meshes to describe the surfaces will be not needed and the analysis convergence will be improved.

2.3.2 contact-search algorithm

In this contact-searching algorithm, only contact nodes, called hitting nodes, on the slave surface are checked against contact segments, the triangular meshes on the master surface, to search out contacting nodes from the slave surface. Therefore, the contact between the nodes on master surface and the slave surface is not taken into account. For a reliable and efficient contact search, in this program, the contact search is performed in two steps: the global search and local search. The Position code algorithm[3] and the inside-outside algorithm[4] are employed for the global search and the local search, respectively.

2.3.3 contact treatment formulation

For the contact problem in the FEM analysis, there are mainly two basic constraint methods to be use. These two methods are the Lagrange multiplier method and the penalty method. In this program, the penalty method is adopted.

In the following formulation, only one hitting point is assumed to come into contact with master surface as shown in Fig 2. To impose the contact constraint condition, a penalty function called contact potential energy function is introduced. Thus, the total potential energy function in (1) is replaced by

$$\begin{aligned} \Phi_P &= \Phi + \pi_P \\ \pi_P &= \frac{1}{2}\alpha G^2 \end{aligned} \tag{9}$$

where α is the penalty constant and $\boldsymbol{G}$ denotes the penetration of the hitting node into target segment that is calculated as

$$G = (\boldsymbol{x}^h - \boldsymbol{x}^{t1}) \cdot \boldsymbol{n} \tag{10}$$

where $\boldsymbol{x}^h$ and $\boldsymbol{x}^{t1}$ are the position vectors of the hitting point and a node of the target segment. $\boldsymbol{n}$ is the normal victor to the target segment.

As Invoking stationary of (9), the variation of the total potential energy can be obtained as follows.

$$\delta\Phi_P = \delta\Phi + \delta\pi_p = \delta\boldsymbol{u}_c^T \cdot (\alpha G \boldsymbol{D}) = \delta\Phi + \delta\boldsymbol{u}_c^T \cdot \boldsymbol{f}_c \tag{11}$$

where, $\boldsymbol{f}_c$ is the contacting force vector, $\boldsymbol{D}$ is a 12×1 matrix and $\boldsymbol{u}$ is the virtual displacement vector as shown below.

$$\delta\boldsymbol{u}_c^T = (\delta u_x^h, \delta u_y^h, \delta u_z^h, \delta u_x^{t1}, \delta u_y^{t1}, \delta u_z^{t1}, \delta u_x^{t2}, \delta u_y^{t2}, \delta u_z^{t2}, \delta u_x^{t3}, \delta u_y^{t3}, \delta u_z^{t3})^T \tag{12}$$

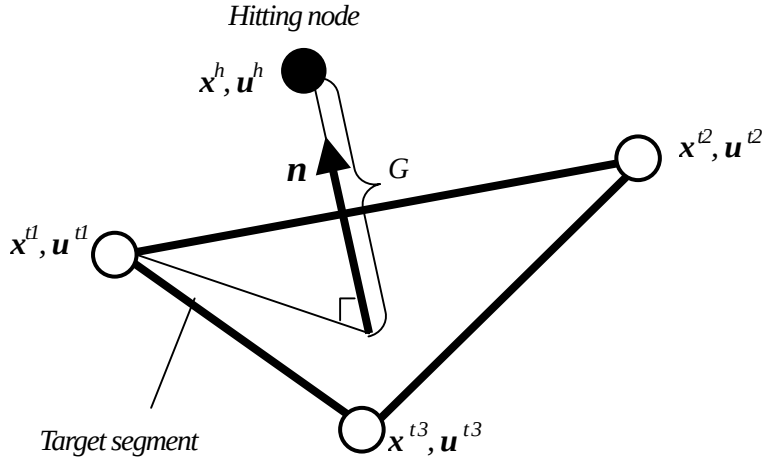

Fig.2 The hitting node and target segment in Contact treatment

Thus, linearizition the equilibrium equations obtained from (11) by using Taylor series expanding and

$$\delta \boldsymbol{f}_c = \boldsymbol{k}_c \delta \boldsymbol{u}_c \tag{13}$$

the global stiffness equation for the contact problem can be finally obtained in the following form.

$$\begin{bmatrix} \boldsymbol{K}_1^{i-1} + \boldsymbol{K}_c^{i-1} & \boldsymbol{K}_2^{i-1} \\ \boldsymbol{K}_3^{i-1} & \boldsymbol{0} \end{bmatrix} \begin{bmatrix} \delta \boldsymbol{U}^i \\ \delta \boldsymbol{\lambda}^i \end{bmatrix} = \begin{bmatrix} \boldsymbol{F}\boldsymbol{U}^{i-1} \\ \boldsymbol{F}\boldsymbol{\lambda}^{i-1} \end{bmatrix} + \begin{bmatrix} \boldsymbol{R} + \boldsymbol{R}_c^{i-1} \\ \boldsymbol{0} \end{bmatrix} \tag{14}$$

where $\boldsymbol{K}_c$ and $\boldsymbol{R}_c$ are induced by contact treatment, which possess nonzero terms only at positions of the hitting node and the nodes of the target segment.

3. SIMULATION OF THE ENCIRCLING SCLERAL BUCKLING OPERATION

The encircling scleral buckling procedure is most frequently applied to clinical treatment of the rhegmatogenous retinal detachment. The rhegmatogeneous retinal detachment is caused by a retina tear generated mainly by liquefaction of the vitreous body, through which liquefied vitreous flow into the space between retina and choriod. The main objective of performing this operation is to close the retina tear by indenting the sclera with a buckle in order to prevent the inflow of the liquefied vitreous. The demand to the numerical simulation from the clinical surgery is thus to simulate the operation procedure and predict the suitable factors for entirely closing the retina tear. To demonstrate the ability of this program to meet such a demand, a simulation of the encircling buckling operation is carried out using an eyeball model described definitely the rhegmatogenous retinal detachment.

3.1 Analysis model and analysis conditions

The analysis model of an eyeball is created based on that used in [2]. Assuming the geometry symmetry, only a half of the eyeball is modeled for simulation. The finite division and tissue division are shown in Fig.3. To describe the rhegmatogenous retinal detachment, the detached retina with a causative tear on it at the top of the eyeball, which is said to most commonly occurs in clinical ophthalmology, is generated and the tear is located on the equator of the eyeball. In this model, 241 linear elastic bar elements and 7421 hexahedral mixed elements are employed to represent the zinn's zonules and the other soft tissues, respectively. The neo-Hooke hyperelastic material model, in which the stored strain energy function is expressed as $W=c(I_1-3)$, is used for all the soft tissues except zinn's zonule, and the material constants are given in Table 1. The buck modulus of 2083.3*MPa* is used for the liquid enclosed within the eyeball.

In this simulation, a buckle shape shown in Fig.4 is used and it is located right above the retina tear. Furthermore, a 8.90*mm* of suture width are adopted.

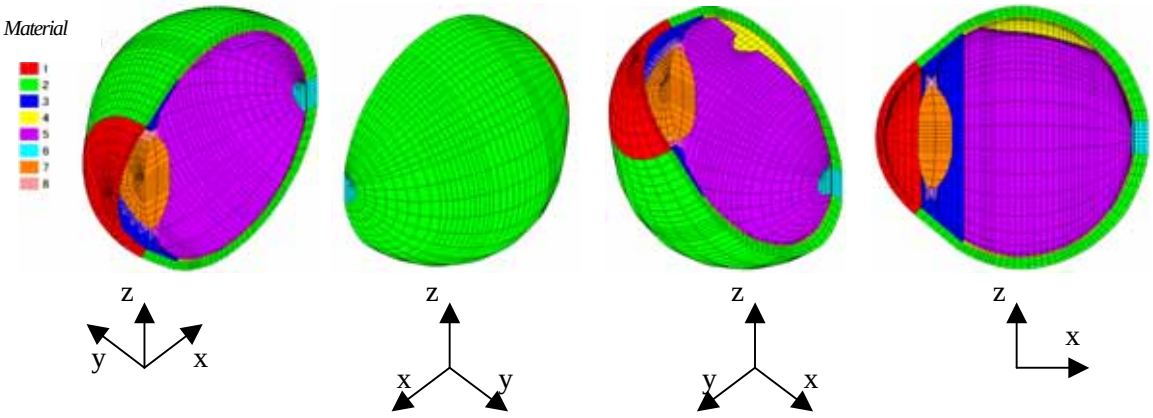

Fig.3 Analysis model for the encircling buckling operation

Table 1 Material constants for soft tissues except zinn's zonules

	cornea-1	sclera-2	ciliary body-3	choroid-4	retina-5	optic nerve-6	lens-7
c	*0.0333*	*0.0833*	*0.01*	*0.0083*	*0.0008*	*0.05*	*10.0*

Zinn's zonules Young's modulus: 100*MPa*

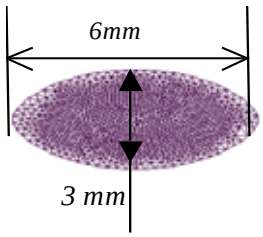

Fig.4 Buckle shape used for the simulation

The simulation is performed in three steps: in the first step, a 15*mmHg* pressure is applied to the inside surfaces of the eyeball as the pressure boundary condition to generate its normal intraocular pressure; in the second and the third steps, the coupling analyses are performed to buckle the eyeball by moving a lot of rigid parts that was imagined as the silicon band and silicon tire in the diametrical directions of the eyeball, and to pursue the sewing process by imposing nodal forces to the suture points.

3.2 Analysis results

The simulation was completed within 20*h* in case of using the Pentium-IV 2*GHz* processor, and the maximum memory needed for calculation was about 600*MB*. It implicates that this 3D coupling analysis program with the newly proposed solid-liquid coupling analysis algorithm is able to carry out an efficient and large-scale analysis required by a practical simulation of the scleral buckling operation procedure.

The simulation results in each calculation step are given in Fig.5. In the second step(buckling process), a weak indenting effect on the sclera , called buckle effect, was obtained, and the detached retina gradually closed to the choriod and finally began to come into contact with it, accompanying to a significant elongation of the optic axis. In the third step(sewing process), then, the anterior of detached retina containing the retina tear thoroughly reattached to the choriod and the retina tear was entirely closed due to a strong buckle effect yielded through sewing. In this step, however, the optic axis changed to degrease and large deformation、serious concentrated stress on the sewing points was locally caused. From the results, it can be seen that the simulation was successfully carried out, and the stress distribution as well as the geometry information including the change in length of the optic axis, the buckle effect, the contact between the retina and choriod and the contact between the buckle and sclera etc. were obtained reasonably.

4. CONCLUSION

In this study, a new algorithm for coupling analysis of the incompressible hyperelastic solid and static liquid was proposed. Using this algorithm, the number of the nonzero terms in the stiffness matrix can be greatly reduced compared to the previous one so that an efficient and large-scale FEM analysis demand from an practical simulation of the sclera buckling operation will become possible. An effective formulation of the contact treatment between deformed bodies which is necessary for treating the reattachment of the detached retina to the choriod and therefore for investigating the conditions of closing the retina tear was also proposed and implemented to the program. Thus, this program has now already possessed all the functions needed for a simulation of the scleral buckling operation as shown in the introduction. In order to demonstrate the capability of this program, then, a encircling buckling operation procedure was carried out using an eyeball model which described definitely the detached retina as well as the retina tear on it and used nearly 10,000 elements. The simulation was successfully performed and, the calculation time and the calculation memory needed for the simulation proved that it was applicable for the practical use. Furthermore, from the simulation, the results of the stress and the results of the deformation including the change in optic axis, the indenting effect etc., especially the reattaching state of the retina to the choriod were obtained reasonably. It can be deduced, therefore, that the suitable factors for a desired retinal buckling operation measured mainly by the effect of closing the retina tear, such as the buckle shape, buckle location, buckling strength, suture width, suture strength and so on, will be predictable by performing a series of simulations under the different factors using this program, prior to the practical surgery.

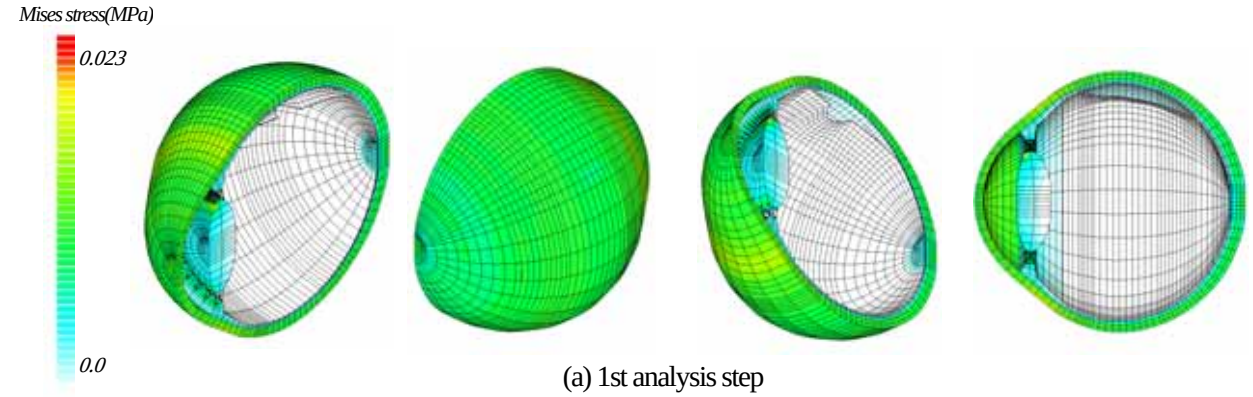

(a) 1st analysis step

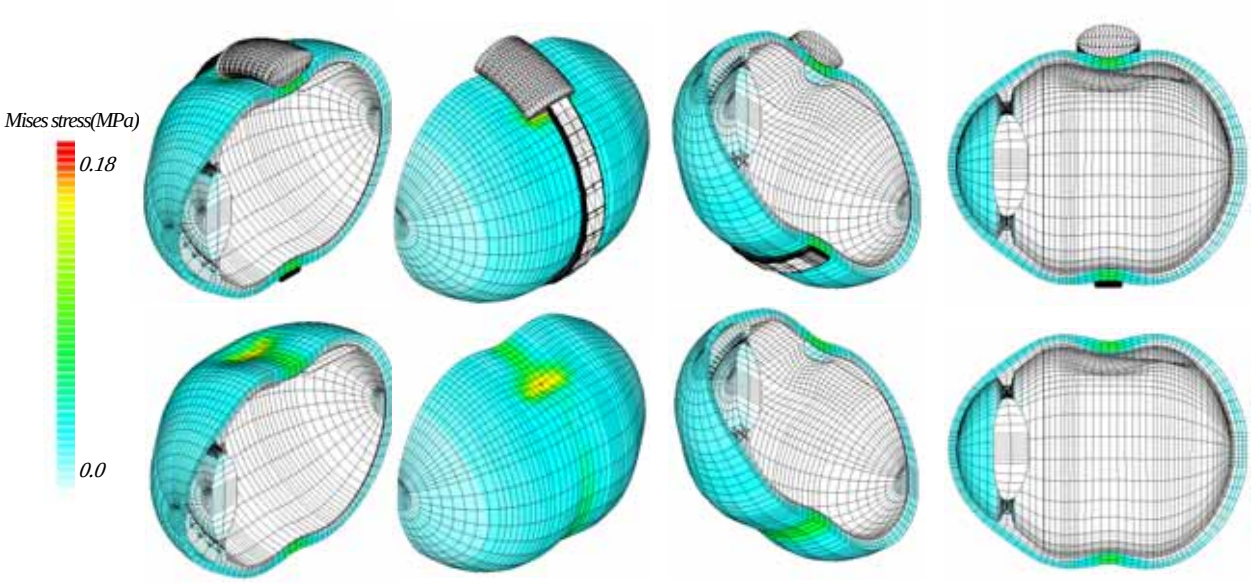

(b) 2nd analysis step(buckling process)

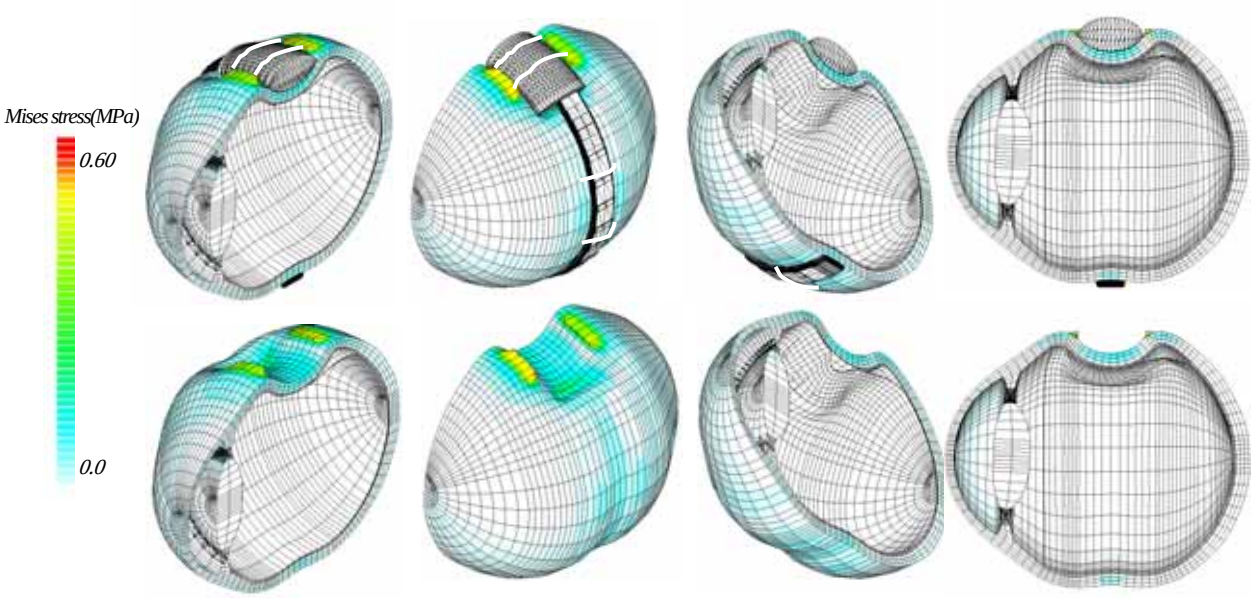

(c) 3rd analysis step(suture process)

Fig.5 Simulation results of the geometry configuration and Mises stress distribution in each analysis step

ACKNOWLEGEMENT

We would like to thank ASTOM R&D(Advanced Simulation Technology of Mechanics R&D, Co. Ltd., RIKEN) for providing us a sparse solver of solving the stiffness equation.

REFERENCE

1. Z.G.Sun and A.Makinouchi, Simulation of Retina Detachment Operation on an eyeball, RIKEN SYMPOSIUM(2001), 18-33. (in Japanese)
2. Z.G.Sun, A.Makinouchi and H.Yabe, Development of a 3D FEM Program for Numerical Simulation of the Retina Detachment Operation on an Eyeball, The 14th Computational Mechanics Conference(2001), 301-302. (in Japanese)
3. M.Oldenburg and L.Nilsson, The Position Code Algorithm for Contact Search, *Int. J. Numer. Mech. Engng.*, **37**, 359-386(1994).
4. S.P.Wang and E.Nakamachi, The Inside-Outside Contact Search Algorithm for Finite Element Analysis, *Int. J. Numer. Mech. Engng.*, **40**, 3665-3685(1997).